Numerical Study of Forced Convection Around a Porous Square Cylinder Using CuO-H₂O Nano-Fluid

Aya Chaibi[1], Salah Guerbaai[2], Houssam Eddine Benchouia[3*], Kamel Meftah[1,4]

[1] Laboratoire de Génie Energétique et Matériaux, LGEM, University Mohamed Khider of Biskra, B.P. 145, Biskra RP 07000, Algeria

[2] Laboratoire de Génie Civil et Hydraulique, Développement durable et Environnement, LARGHYDE, University Mohamed Khider of Biskra, Biskra RP 07000, Algeria

[3] Laboratoire de Génie Mécanique, LGM, University Mohamed Khider of Biskra, Biskra RP 07000, Algeria

[4] Faculty of Technology, University of Batna 2, Batna 05078, Algeria

Corresponding Author Email: houssam.benchouia@univ-biskra.dz

ABSTRACT

In this research, a numerical analysis of the flow was performed occurring through the square porous cylinder situated between two parallel surfaces and maintaining a consistent temperature, where the Nano-fluid was subjected to forced convection and consisted of copper oxide particles suspended in water in the form of particles, all in a two-dimensional state. The transport equations are numerically fixed through the finite volume approach, and the SIMPLE algorithm is employed for velocity-pressure coupling. Numerical results are provided for the ranges $5 \leq Re \leq 40$, $0 \leq \emptyset \leq 10\%$, $10^{-6} \leq Da \leq 10^{-2}$, with a blocking ratio $\varphi = b/H = 1/8$. The streamlines, isotherms, variations in the Nusselt number, and drag coefficient are illustrated to assess the influence of a variety of parameters on the framework of fluid flow and heat exchange. The recirculation zone's dimensions and heat transmission were found to rise with rising Reynolds number and nanoparticle volume concentration, particularly pronounced at elevated Darcy numbers. The drag coefficient reduces as the Reynolds number boosts, and it increases as the nanoparticle volume fraction rises as well.

1. INTRODUCTION

Studies on the flow of various incompressible fluids around and through unprofiled bodies made of different materials and confined between two walls have gained significant importance in recent years [1, 2]. This is due to their contribution to solving technical issues and helping engineers better understand the various phenomena associated with these flows. This information is crucial for the construction of many structures, including drying processes, nuclear reactors, thermal insulation, electrical gadgets, and cooling towers.

Many studies have examined turbulent and laminar heat transmission in ducts designed with both circular and non-circular cross-sections, such as sinusoidal configurations, elliptical, hexagonal, trapezoidal, rectangular, and triangular [3, 4].

In recent years, the dynamics of fluxes inside and through porous media have become increasingly significant [5-7]. Modeling these systems is difficult because of material permeability. Consequently, numerical simulation and modeling of these processes are essential, enabling researchers to understand and elucidate physical phenomena [8]. The incompressible fluid was tested with a blockage ratio of 1/8 so that the flow was finite through a square cylinder using the MVF and LBA computational methods. Gupta et al. [9]

studied the blockage case with a ratio φ=1/20 in the case of the cylinder when it is square, and that is when the fluid that is not Newtonian flows, and in the case of forced convection, and that is to study the heat transfer. Paliwal et al. [10] studied unconfined flow with φ=1/15 blockage ratio, whereas Dhiman et al. [11] studied an insulated cylinder. Fluid dynamics and heat conduction are affected by several factors. Dhiman et al. [12] examined the impact of Reynolds and Prandtl values on the thermal transfer properties of a solitary square cylinder. Sharma et al. [13] examine a mix of convection flow and heat transfer in the vicinity of a long cylinder with a square cross-section, influenced by assisting buoyancy in a vertical unconfined arrangement. Yu et al. [14] investigate the presence of downstream recirculation cells, noting that their intensity is formed by variables such as the Reynolds number and the Darcy number in flow via a square permeable cylinder. Wu and Wang [15] examined an unstable flow with forced heat transmission by convection through a square cylinder within a conduit containing a heat source. Dhinakaran and Ponmozhi [16] investigated the transfer of heat in a constant-temperature porous square cylinder.

The Darcy and Reynolds numbers influenced the flow pattern surrounding the cylinder. Fluid with low Darcy values traverses a solid square cylinder. Vijaybabu et al. [17] studied thermal buoyancy-driven mixed convection heat transport in

an unconfined porous square cylinder using a mesoscopic technique. Numerical experiments using the Lattice Boltzmann method utilizing two distribution functions.

Many heat transfer techniques use water, ethylene glycol, propylene glycol, and oils. Nanoparticles with 1-100 mm diameters and more excellent thermal conductivity are uniformly distributed and suspended in the working fluid to create a stable Nano-fluid to improve heat transfer.

Nano-fluids improve heat transfer fluid thermal conductivity by stabilizing dispersion, enhancing surface-to-volume ratio, and decreasing particle clogging. Nano-fluid selection for a heat transfer application significantly affects thermal system efficiency [18-20]. Azzawi et al. [4], found that Nano-fluids like Al_2O_3/Water can boost heat transmission by 15%. Nanoparticle concentrations increase improvements even more. Low-porous foams increase heat transmission by providing a more contact surface. Etminan-Farooji et al. [21] comparative study of several Nano-fluids with conventional fluids in forced convection when these Nano-fluids flow through a square cylinder ($\varphi=1/20$), all as a numerical study.

Copper oxide (CuO) is being studied for its affordability, low energy band gap, and versatility in gas sensors, solar cells, lithium-ion batteries, and photo-catalysts. This material can be precisely tuned for optical, electrical, and magnetic properties by adding metals. Thus, advanced technological applications depend on it [5, 22]. Nano-fluids with CuO nanoparticles improve thermal conductivity and heat transmission, making them essential for cooling systems and energy conservation. CuO is important in commercial applications and cutting-edge research due to its meticulous form manipulation utilizing multiple synthesis methods [19, 23]. Recent research suggests that CuO Nano-fluid can improve refrigeration system heat transfer and performance. CuO–Jatropha oil Nano-fluids improved thermal conductivity by 9% at 2% concentration and 323 K, according to Gobane et al. [24]. Transfer of heat and the flow of fluid within a porous container with a sophisticated construction were studied by Sheikholeslami and Rokni [25]. The enclosure had magneto hydrodynamic field-exposed CuO water Nano-fluid. The temperature gradient decreased as Hartman's number increased.

Despite the numerous studies in this field, certain cases that have not yet been studied still warrant investigation, as they could help researchers understand the developments of fluid flow past and around bodies such as a square cylinder.

The study mainly investigates the relationship between particle volume fraction and Reynolds number in thermal conductivity and flow dynamics. The used fluid is a nanofluid consisting of Water/Copper oxide, subjected to forced convection and passing through a porous square cylinder positioned among two aligned slabs using shielding ratio $\varphi = 1/8$. This study's value resides in its thorough approach. This numerical study presents an in-depth analysis, delivering a thorough overview of the behavior of CuO/Water Nano-fluids by investigating various Reynolds numbers, nanoparticle concentrations, and Darcy numbers. The results are displayed using streamlines, isotherms, and fluctuations in the Nusselt number and drag coefficient.

2. PHYSICAL ISSUE AND MATHEMATICAL FORMULATION

Figure 1 illustrates a geometrical representation that is currently being examined. A cross-section of a square porous cylinder is held at a constant temperature T_p, which is elevated above the ambient temperature T_0 and is subjected to a flow of a Nano-fluid consisting of water and CuO, positioned between two parallel plates. The cylinder transfers heat to the surrounding fluid. The channel's dimensions are identical to those analyzed by Dhiman et al. [12].
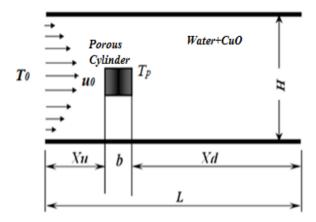

Figure 1. Problem geometry

The Nano-fluid inside the channel is Newtonian and incompressible. The non-dimensional representations of the continuous equation, with the X and Y elements of the heat energy equation together with the formulas of Navier-Stokes, for the passage of fluid through a square cylinder assuming negligible dissipation with unchanged physical and thermal properties in the two-dimensional case are as follows:

The continuum equation:

$$\frac{\partial U}{\partial X} + \frac{\partial V}{\partial Y} = 0 \tag{1}$$

The momentum formula:
In the X direction:

$$\frac{1}{\varepsilon}\left(\frac{\partial(U.U)}{\partial X} + \frac{\partial(V.U)}{\partial Y}\right)$$
$$= -\varepsilon\frac{\rho_f}{\rho_{nf}}\frac{\partial P}{\partial X} + \frac{1}{v_f.Re}\frac{\mu_{eff}}{\rho_{nf}}\left(\frac{\partial^2 U}{\partial X^2} + \frac{\partial^2 U}{\partial Y^2}\right)$$
$$- C\left(\varepsilon\frac{v_{nf}}{v_f ReDa}U \right.$$
$$\left. + \frac{1.75}{\sqrt{150}}\frac{1}{\sqrt{Da}} \times \frac{\sqrt{U^2+V^2}}{\sqrt{\varepsilon}}U\right) \tag{2}$$

In the Y direction:

$$\frac{1}{\varepsilon}\left(\frac{\partial(U.V)}{\partial X} + \frac{\partial(V.V)}{\partial Y}\right) = -\varepsilon\frac{\rho_f}{\rho_{nf}}\frac{\partial P}{\partial Y} + \frac{1}{v_f.Re}\frac{\mu_{eff}}{\rho_{nf}}\left(\frac{\partial^2 V}{\partial X^2} + \frac{\partial^2 V}{\partial Y^2}\right)$$
$$- C\left(\varepsilon\frac{v_{nf}}{v_f ReDa}V\right.$$
$$\left. + \frac{1.75}{\sqrt{150}}\frac{1}{\sqrt{Da}} \times \frac{\sqrt{U^2+V^2}}{\sqrt{\varepsilon}}V\right) \tag{3}$$

Energy equation:

$$\frac{1}{\varepsilon}\left(\frac{\partial(U.\theta)}{\partial X} + \frac{\partial(V.\theta)}{\partial Y}\right) = \frac{\alpha_{nf}}{\alpha_f}\frac{R_k}{Re.Pr}\left(\frac{\partial^2\theta}{\partial X^2} + \frac{\partial^2\theta}{\partial Y^2}\right) \tag{4}$$

$$C = \begin{cases} 0. & \text{external to the permeable medea} \\ 1. & \text{in the porous medium} \end{cases} \tag{5}$$

$$\varepsilon = \begin{cases} 1, & external\ to\ the\ permeable\ medea \\ 0 < \epsilon < 1, & in\ the\ porous\ medium \end{cases} \quad (6)$$

Variables that are marked as dimensionless are characterized as follows:

$$X = \frac{x}{b}, Y = \frac{y}{b}, U = \frac{u}{u_0}, V = \frac{v}{u_0}, P = \frac{p}{\rho_f u_0^2}, and\ \theta\ \frac{T - T_0}{\Delta T} \quad (7)$$

So that the following boundary conditions are regarded as:
In $Y = 0$ and $Y = 1$ for $0 \leq X \leq L/b$;

$$U = V = \frac{\partial \theta}{\partial Y} = 0 \quad (8)$$

At the channel inlet $= 1 - (2\varphi Y)^2$;

$$V = \theta = 0 \quad (9)$$

At channel end,

$$\frac{\partial U}{\partial X} = \frac{\partial V}{\partial X} = \frac{\partial \theta}{\partial X} = 0 \quad (10)$$

In fluid-porous media interaction,

$$\frac{\partial U}{\partial n}\bigg|_{Fluid} = \frac{1}{\varepsilon} \frac{\partial U}{\partial n}\bigg|_{Porous\ Medium}$$

And,

$$\frac{\partial V}{\partial n}\bigg|_{Fluid} = \frac{1}{\varepsilon} \frac{\partial V}{\partial n}\bigg|_{Porous\ Medium} \quad (11)$$

The Nusselt number at the local level was calculated and expressed to evaluate the improvement for the cylinder characterized as porous when the fluid flows through it, as follows:

$$Nu = -\frac{k_{eff}}{k_{nf}} \frac{\partial \theta}{\partial n}\bigg|_{Along\ the\ Cylinder's\ Surface} \quad (12)$$

n: Denotes the orientations perpendicular to the cylindrical surface; The mean Nusselt number $\overline{Nu} = \frac{1}{s}\int_0^s Nu ds$
$ds=dx$ along the vertical wall;
$ds=dy$ along the horizontal wall;
The drag coefficient can be evaluated as follows:

$$C_D = C_{DF} + C_{DP} \quad (13)$$

With:

$$C_{DF} = \frac{2.0}{Re} \frac{\mu_{eff}}{\mu_f} \frac{\rho_f}{\rho_{nf}} \int \left[\left(\frac{\partial U}{\partial Y}\right)_{lower\ face} + \left(\frac{\partial U}{\partial Y}\right)_{upper\ face.} \right] dX \quad (14)$$

And,

$$C_{DP} = \int [P_{front\ face} - P_{rear\ face}] d \quad (15)$$

3. RESOLUTION METHODS

The finite volume approach quantitatively resolves the momentum and energy equations [26]. The SIMPLE technique integrates momentum equations with continuity.

Using the power law, diffusion and convection are separated as terms by following this common approach.

The mesh employed is non-uniform in both dimensions (X, Y). The thickness is reduced toward the walls of the square cylinder, where considerable variations in velocity and temperature gradients are anticipated. A test was conducted to ascertain the independence of the numeric solution's grid size, utilizing grid configurations from 200×100 to 330×230 for the laminar flow of a Nano-fluid with a nanoparticle concentration of Ø=0.04 surrounding an impermeable square cylinder (Da=10-17). The test outcomes are displayed in Table 1. The largest relative error between the solutions of 288×186 and 330×230 for computing the average Nusselt number and the coefficient of drag is lower than 1.4%. To optimize the computational time, a grid system 288×186 was deemed sufficiently accurate and chosen for all calculations. Convergence of this iterative procedure is achieved when:

$$Max((\Phi_{i,j}^{k+1} - \Phi_{i,j}^k)/\Phi_{i,j}^{k+1}) \leq 10^{-5} \quad (16)$$

With, $\Phi_{i,j}^{k+1}$ is U, V, or θ at each position (X_i, Y_j) of the separated domain at iteration k.

Table 1. Grid independency study (Re=20, ϕ=4%)

$N_x \times N_y$	$\overline{Nu}$	Percentage Change	Total Drag Coefficient C_D	Percentage Change
200×100	4.59	2.61	2.53	2.76
250×150	4.47	2.01	2.46	0.81
288×186	4.38	1.36	2.44	0.41
330×230	4.32	-	2.43	-

3.1 Code validation

We confirm the FORTRAN code by comparing our results with their of Dhiman et al. [12] for restricted square cylinders with φ=1/8, as shown in Table 2, and Sharma and Eswaran [27], for unconfined square cylinders with φ=1/20, as shown in Table 3.

Table 2. Comparing CD and L results with those reported by Dhiman et al. [12]

Re	20		30		40	
	L_r	C_D	L_r	C_D	L_r	C_D
Present work	1.08	2.44	1.68	2.02	2.23	1.79
Dhiman et al. [12]	1.05	2.44	1.62	1.99	2.17	1.75

The findings of this study are in complete concordance with existing literature.

Table 3. $\overline{Nu}$ and L_r values and comparison with those of Sharma and Eswaran [27]

Re	20		30		40	
	L_r	$\overline{Nu}$	L_r	$\overline{Nu}$	L_r	$\overline{Nu}$
Present work	1.36	2.13	2.10	2.52	2.74	2.86
Sharma and Eswaran [27]	1.34	2.05	2.07	2.41	2.82	2.71

4. RESULTS AND DISCUSSION

Numerical computations were executed for a laminar and stable flow of Nano-fluid (Water+CuO) via a square porous

cylinder between two parallel plates. Reynolds numbers ranged from 5 to 40, and volume fractions from 0 to 10%. Table 4 lists base fluid and nanoparticle thermophysical properties. The viscosity that is effectual, density, Heating conductivity, and thermal diffusivity of the Nano-fluid are represented by the following equations:

$$\mu_{eff} = \frac{\mu_f}{(1-\emptyset)^{2.5}} \qquad (17)$$

$$\rho_{nf} = \emptyset \rho_s + (1-\emptyset)\rho_f \qquad (18)$$

$$k_{eff} = k_f \frac{(k_s + 2k_f) - 2\emptyset(k_f - k_s)}{(k_s + 2k_f) + \emptyset(k_f - k_s)} \qquad (19)$$

$$\alpha_{nf} = \frac{k_{eff}}{(\rho Cp)_{nf}} \qquad (20)$$

$$(\rho Cp)_{nf} = \emptyset(\rho Cp)_s + (1-\emptyset)(\rho Cp)_f \qquad (21)$$
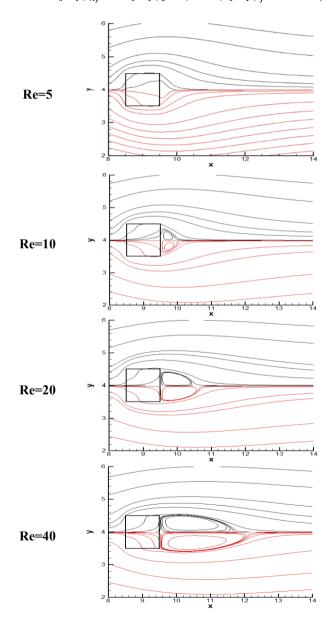

Figure 2. Streamlines that traverse the cylinder for various Reynolds number amounts (5, 10, 20, and 40) upper half for water and lower half for Nano-fluid with Da=10⁻³, ε=0.977, and Ø=10%

Table 4. Thermophysical characteristics of the reference fluid and nanoparticles

Properties	Pure Water	CuO
ρ (Kg/m³)	995.7	6350
k (W/m K)	0.6	76.5
C_p (J/kg K)	4183	535.6
μ (Pa.s).10⁻⁴	7.975	-

The flow patterns surrounding the porous square cylinder, depicted in Figure 2, demonstrate the emergence of a recirculation zone consisting of two symmetrical cells, whose dimensions expand with the Reynolds number. This behavior is ascribed to the predominance of inertial forces at elevated Reynolds numbers, promoting flow separation. Utilizing a CuO-H_2O Nano-fluid (Ø=10%) results in early flow separation, with the center of the recirculation cell relocating further from the cylinder's surface in comparison to the base fluid (Water). This change is probably attributable to the improved thermo-physical characteristics of the Nano-fluid. Figure 3 illustrates the variation in the extent of the recirculation zone.
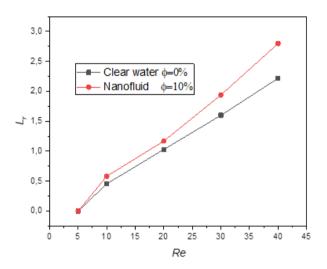

Figure 3. Variation in cell length with Reynolds number at Ø=0% and Ø=10%

Figure 4 depicts the isotherms surrounding the square cylinder for varying Reynolds values. The upper and lower sections display the isotherms for water and the Water/CuO Nano-fluid, respectively. Both fluids demonstrate a comparable trend; however, the Nano-fluid shows a markedly superior heat transfer capability from the cylinder. The isotherms on the cylinder's front surface are densely arranged, signifying pronounced temperature gradients and an elevated heat transfer rate in these regions. With an increase in the Reynolds number, the isotherms progressively migrate towards the rear face of the cylinder as a result of enhanced recirculation cells, leading to effective transverse heat dispersion due to energy conservation.

Figure 5 depicts the effect of nanoparticles on the drag coefficient. The results for various Reynolds numbers indicate a nonlinear reduction in the drag coefficient as the Reynolds number increases, attributable to the enhancement of shear forces. With an increase in the volumetric concentration of nanoparticles, the effective viscosity and density of the Nano-fluid elevate correspondingly. The nanoparticles modify the fluid's structure owing to their size and characteristics, hence enhancing its viscosity. As a result,

this causes the dissipation of kinetic energy in the fluid adjacent to the wall, impacting the boundary layer and elevating the drag coefficient.
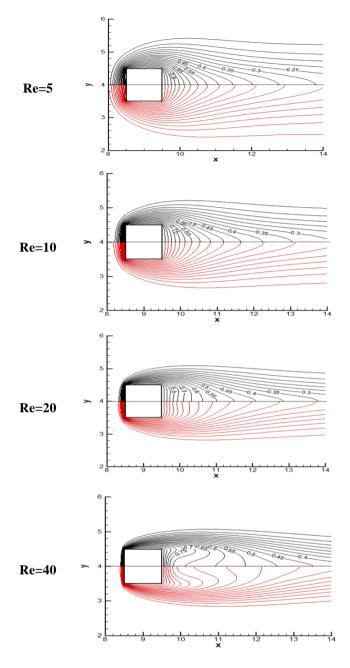

Figure 4. Isotherms around the cylinder for different Reynolds number values (5,10,20 and 40) upper half for water and lower half for Nano-fluid with Da=10⁻³, ε=0.977 and Ø=10%

Figure 6 illustrates the correlation between the Reynolds number and the mean Nusselt number for a Nano-fluid (water/CuO) with differing nanoparticle volume fractions under forced convection circumstances. This image illustrates a notable trend wherein the average Nusselt number increases with rising Reynolds numbers and nanoparticle volume fractions. The enhancement in heat exchange efficiency results from the integration of CuO nanoparticles, which markedly improves the thermal conductivity of the Nano-fluid.

As the Reynolds number rises, the strength of recirculation cells escalates, leading to enhanced convective heat transfer from the porous square cylinder. Likewise, augmenting the concentration of nanoparticles in the Nano-fluid improves

thermal conductivity.

Figure 7 illustrates the impact of Darcy number fluctuation on the flow structure. At low Darcy numbers, the cylinder exhibits low permeability and fluid penetration into the porous body is slow, forming a recirculation zone downstream. As the Darcy number increases, fluid penetration into the porous medium becomes more manageable, and flow resistance decreases. The fluid propagates more quickly through the porous body, reducing the recirculation cells' intensity, eventually disappearing entirely at high Darcy numbers.
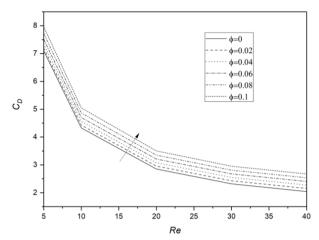

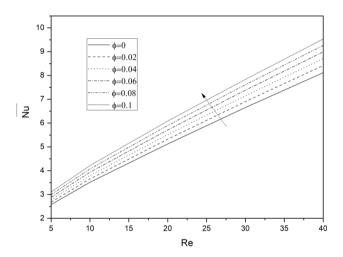**Figure 5.** Different values φ in the case of Reynolds number vs drag coefficient

Figure 6. Average Nusselt number as influenced by Reynolds number for various values of Ø

Figure 8 illustrates the isotherms surrounding the porous square cylinder at Re=30 for various Darcy number values. At low Darcy number levels, the fluid predominantly circulates the square cylinder, which functions as a solid, impermeable entity. With an increase in the Darcy number, the fluid begins to infiltrate the square cylinder, augmenting the heat transfer surface area and thus enhancing thermal exchange efficiency.

Figure 9 illustrates the fluctuation of the mean Nusselt number along the porous square cylinder about the Darcy number for Re=30. The Nusselt number exhibits a modest growth for Darcy's number below 10⁻⁴, followed by an exponential rise thereafter. Because the thermal proprieties of Nano-fluids, such as conductivity and thermal diffusivity, increase with the volume fraction, one can also see that the Nusselt number increases with the volume fraction.
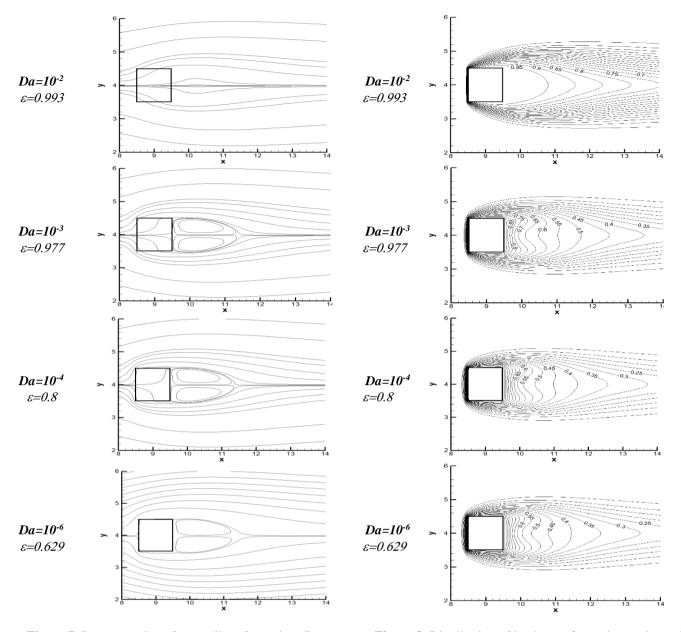
Figure 7. Representation of streamlines for various Darcy number values, with Re=30 and Ø=10%

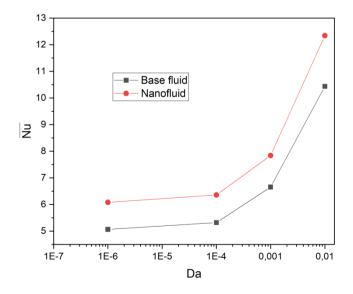**Figure 8.** Distribution of isotherms for various values of Darcy number, where Ø=10%, and Re=30

Figure 9. Variation of average Nusselt number with Darcy number at Re=30, Ø=0% (Base fluid) Ø=10% (Nano-fluid)

5. CONCLUSIONS

This study computationally solves the equations governing the flow of a Nano-fluid (CuO+Water) and heat transfer through forced convection from a porous square cylinder situated between two parallel plates, kept at a constant temperature, using the finite volume approach.

The objective is to examine the influence of different parameters defining the fluid and the square cylinder, including nanoparticle volumetric concentration ϕ, Reynolds number Re, and square cylinder permeability Da, on the flow structure and heat transmission. From the results acquired, we may deduce that:

- The length of the recirculation cells behind the porous cylinder grows with the Reynolds number and is further augmented by an increase in nanoparticle volumetric concentration. As the Reynolds number diminishes, viscous forces gain prominence, resulting in an elevated drag coefficient;

- As the Darcy number rises, fluid movement through the porous medium becomes more efficient, resulting in a

reduction of the intensity of the recirculation cells. The rate of heat transfer, represented by the Nusselt number (Nu), markedly increases with higher nanoparticle volume fractions. This enhancement results from the improved thermal conductivity of the Nano-fluid, which promotes more effective heat transfer from the square cylinder to the fluid;

- The heat transfer rate experiences a modest increase for Darcy numbers below 10^{-4} and an exponential rise for Darcy numbers over 10^{-4}, underscoring the pivotal influence of permeability on thermal performance.

The results emphasize the capability of CuO-H_2O Nano-fluids to significantly enhance heat transfer efficiency in many engineering fields, including electronic cooling systems, automotive and aerospace engineering, and industrial heat exchangers. Future research could further investigate factors like particle shape, temperature-dependent properties, and transient flow conditions to optimize Nano-fluid applications.

REFERENCES

[1] Khalaf, A.F., Basem, A., Hussein, H.Q., Jasim, A.K., Hammoodi, K.A., Al-Tajer, A.M., Omer, I., Flayyih, M.A. (2022). Improvement of heat transfer by using porous media, nanofluid, and fins: A review. International Journal of Heat and Technology, 40(2): 497-521. https://doi.org/10.18280/ijht.400218

[2] Alazmi, B., Vafai, K. (2001). Analysis of fluid flow and heat transfer interfacial conditions between a porous medium and a fluid layer. International Journal of Heat and Mass Transfer, 44(9): 1735-1749. https://doi.org/10.1016/S0017-9310(00)00217-9

[3] Alshuraiaan, B. (2022). Mixed convection flow and heat transfer of two rotating cylinders in a trapezoidal enclosure filled with porous medium. International Journal of Heat and Technology, 40(6): 1500-1506. https://doi.org/10.18280/ijht.400619

[4] Azzawi, I.D.J., Yahya, S.G., Al-Rubaye, L.A.H., Ali, S.K. (2021). Heat transfer enhancement of different channel geometries using nanofluids and porous media. International Journal of Heat and Technology, 39(4): 1197-1206. https://doi.org/10.18280/ijht.390417

[5] Bagyalakshmi, S., Subash, M., Uthrakumar, R., Aravindan, S., Kaviyarasu, K. (2024). Highly absorption and an excellent optical bandgap of CuO doped Fe nanoparticles for advanced photocatalytic applications. Digest Journal of Nanomaterials and Biostructures, 19(1): 201-211. https://doi.org/10.15251/DJNB.2024.191.201

[6] Belhadj, M., Atia, A., Benchatti, A. (2020). Analysis of natural convection in porous media for thermal storage using Darcy-Brinkman-Forcheimer formulation. Mathematical Modelling of Engineering Problems, 7(1): 73-78. https://doi.org/10.18280/mmep.070109

[7] Brahmi, C.E., Battira, M.M., Belghar, N., Kalfali, M., Driss, Z. (2024). Free convection inside greenhouse cavity partially filled with bottom porous layer: The influence of soil's porosity and permeability. International Journal of Heat and Technology, 42(6): 1849-1858. https://doi.org/10.18280/ijht.420602

[8] Breuer, M., Bernsdorf, J., Zeiser, T., Durst, F. (2000). Accurate computations of the laminar flow past a square cylinder based on two different methods: Lattice-Boltzmann and finite-volume. International Journal of Heat and Fluid Flow, 21(2): 186-196. https://doi.org/https://doi.org/10.1016/S0142-727X(99)00081-8

[9] Gupta, A.K., Sharma, A., Chhabra, R.P., Eswaran, V. (2003). Two-dimensional steady flow of a power-law fluid past a square cylinder in a plane channel: Momentum and heat-transfer characteristics. Industrial & Engineering Chemistry Research, 42(22): 5674–5686. https://doi.org/10.1021/ie030368f

[10] Paliwal, B., Sharma, A., Chhabra, R.P., Eswaran, V. (2003). Power law fluid flow past a square cylinder: Momentum and heat transfer characteristics. Chemical Engineering Science, 58(23-24): 5315-5329. https://doi.org/10.1016/j.ces.2003.09.010

[11] Dhiman, A.K., Chhabra, R.P., Sharma, A., Eswaran, V. (2006). Effects of Reynolds and Prandtl numbers on heat transfer across a square cylinder in the steady flow regime. Numerical Heat Transfer, Part A: Applications, 49(7): 717-731. http://doi.org/10.1080/10407780500283325

[12] Dhiman, A.K., Chhabra, R.P., Eswaran, V. (2006). Steady flow of power-law fluids across a square cylinder. Chemical Engineering Research and Design, 84(4): 300-310. https://doi.org/10.1205/cherd05017

[13] Sharma, N., Dhiman, A.K., Kumar, S. (2012). Mixed convection flow and heat transfer across a square cylinder under the influence of aiding buoyancy at low Reynolds numbers. International Journal of Heat and Mass Transfer, 55(9-10): 2601-2614. https://doi.org/10.1016/j.ijheatmasstransfer.2011.12.034

[14] Yu, P., Zeng, Y., Lee, T.S., Bai, H.X., Low, H.T. (2010). Wake structure for flow past and through a porous square cylinder. International Journal of Heat and Fluid Flow, 31(2): 141-153. https://doi.org/10.1016/j.ijheatfluidflow.2009.12.009

[15] Wu, H.W., Wang, R.H. (2010). Convective heat transfer over a heated square porous cylinder in a channel. International Journal of Heat and Mass Transfer, 53(9-10): 1927-1937. https://doi.org/10.1016/j.ijheatmasstransfer.2009.12.063

[16] Dhinakaran, S., Ponmozhi, J. (2011). Heat transfer from a permeable square cylinder to a flowing fluid. Energy Conversion and Management, 52(5): 2170-2182. https://doi.org/10.1016/j.enconman.2010.12.027

[17] Vijaybabu, T.R., Anirudh, K., Dhinakaran, S. (2017). Mixed convective heat transfer from a permeable square cylinder: A lattice Boltzmann analysis. International Journal of Heat and Mass Transfer, 115: 854-870. https://doi.org/10.1016/j.ijheatmasstransfer.2017.08.033

[18] Palanisamy, R., Parthipan, G., Palani, S. (2021). Study of synthesis, characterization and thermo physical properties of Al_2O_3-SiO_2-TiO_2/H_2O based tri-hybrid nanofluid. Digest Journal of Nanomaterials and Biostructures, 16(3): 16939-16949. https://doi.org/10.15251/djnb.2021.163.939

[19] Iqbal, S.M., Raj, C.S., Michael, J.J., Irfan, A.M. (2017). A comparative investigation of Al_2O_3/H_2O, SiO_2/H_2O

And ZrO$_2$/H$_2$O nanofluid for heat transfer applications. Digest Journal of Nanomaterials & Biostructures (DJNB), 12(2): 255-263.

[20] Cui, W., Shen, Z., Yang, J., Wu, S. (2015). Flow and heat transfer behaviors of water-based nanofluids confined in nanochannel by molecular dynamics simulation. Digest Journal of Nanomaterials and Biostructures, 10(2): 401-413.

[21] Etminan-Farooji, V., Ebrahimnia-Bajestan, E., Niazmand, H., Wongwises, S. (2012). Unconfined laminar nanofluid flow and heat transfer around a square cylinder. International Journal of Heat and Mass Transfer, 55(5-6): 1475-1485. https://doi.org/10.1016/j.ijheatmasstransfer.2011.10.030

[22] Mazhar, M.E., Asif, R., Waheed, A., Ahmad, J., Usmani, M.N., Syed, I., Khan, H.M., Ahmad, I., Naz, R., Ahmad, S., Abbas, W., Mahmood, M. (2020). Electrochemical sensing of H$_2$O$_2$ by hydrothermally synthesized pure copper oxide materials. Digest Journal of Nanomaterials and Biostructures, 15(4): 1239-1245. https://doi.org/10.15251/djnb.2020.154.1239

[23] S. Senthilraja, K. Vijayakumar, R. Gangadevi, A comparative study on thermal conductivity of Al$_2$O$_3$/water, CuO/water and Al$_2$O$_3$–CuO/water nanofluids. Digest Journal of Nanomaterials and Biostructures, 10(4): 1449-1458.

[24] Gobane, S., Dama, T., Hasan, N., Yanmaz, E. (2023). Characterization of copper oxide-Jatropha oil nanofluid as a secondary refrigerant. Journal of Nanomaterials, 2023(1): 7612959. https://doi.org/10.1155/2023/7612959

[25] Sheikholeslami, M., Rokni, H.B. (2017). Magnetohydrodynamic CuO–water nanofluid in a porous complex-shaped enclosure. Journal of Thermal Science and Engineering Applications, 9(4): 41007. https://doi.org/10.1115/1.4035973

[26] Patankar, S. (1980). Numerical Heat Transfer and Fluid Flow (1st ed.). CRC Press. https://doi.org/10.1201/9781482234213

[27] Sharma, A., Eswaran, V. (2004). Heat and fluid flow across a square cylinder in the two-dimensional laminar flow regime. Numerical Heat Transfer, Part A: Applications, 45(3): 247-269. https://doi.org/10.1080/10407780490278562

NOMENCLATURE

b	side of the square, m
CDf	friction drag coefficient
CDP	pressure drag coefficient
CD	drag coefficient
g	gravity acceleration
H	width of the study area, m
k	thermal conductivity, W/m·k
L	length of study area, m
Nu	Nusselt number
$\overline{Nu}$	average Nusselt number
P	dimensionless pressure
Pr	Prandtl number
Re	Reynolds number
T	Temperature, k
θ	dimensionless temperature
u, v	velocity components in x, and y directions, respectively, m/s
U, V	dimensionless velocity components
x, y	dimensional cartesian coordinates, m
X, Y	dimensionless cartesian coordinates

Greek letters

Λ	viscosity ratio, μ_{eff}/μ_f
μ	dynamic viscosity, pa.s
ρ	fluid density, Kg/m^3
φ	blockage ratio, b/h
Ø	particle volumetric concentration, %
α	thermal diffusivity, m^2/s
ν	kinematic viscosity, m/s
κ	material permeability, m^2
ε	porosity

Subscript

f	fluid
s	solid
nf	nano-fluid
eff	effective
0	entry condition